

## Development of a positron-imaging detector with background rejection capability

Seiichi YAMAMOTO,<sup>\*,\*\*\*</sup> Tatsuya HIGASHI,<sup>\*\*</sup> Keiichi MATSUMOTO<sup>\*\*\*</sup> and Michio SENDA<sup>\*\*\*</sup>

<sup>\*</sup>*Department of Electrical Engineering, Kobe City College of Technology*

<sup>\*\*</sup>*Department of Diagnostic Imaging & Nuclear Medicine, Kyoto University Graduate School of Medicine*

<sup>\*\*\*</sup>*Department of Molecular Imaging, Institute of Biomedical Research and Innovation*

**Objective:** Intra-operative probes have recently become important instruments in nuclear medicine. In such an application, the radiopharmaceutical F-18-fluorodeoxyglucose (FDG) is promising. For the FDG-guided surgery, we developed and tested a positron-imaging detector with background rejection capability. **Methods:** The detector consists of an array of phoswich scintillators, a multi-channel position-sensitive photo-multiplier tube (PSPMT) and an electronic circuit. The scintillators and the PSPMT are encased in a tungsten shield and replaceable collimators are mounted on the top of the detector. Positrons are detected by the plastic scintillators while annihilation photons are detected by the BGOs. By employing a pulse-shape analysis, we can distinguish the true events (positrons) from background gamma events. The dimensions of each plastic scintillator are 2 mm × 2 mm × 3 mm and those of the BGO are 2 mm × 2 mm × 15 mm. These scintillators are optically coupled to each other and combined in an 8 × 8 array, which is optically coupled to a 1-inch square 8 × 8 multi-channel PSPMT via optical fibers. Position determination of the positrons is performed by 64-channel threshold circuits while the pulse shape analysis is applied for the summing signal. **Results:** The spatial resolution was measured by positioning an F-18 point source onto one pixel of the detector and found that the spillover to the neighbor pixel was less than 20%. The background count rate was less than 2 cps for a 20-cm diameter, 20-cm long cylinder phantom containing 3.7 MBq of F-18. **Conclusion:** These results indicated that the developed positron-imaging detector will be useful for FDG-guided surgery.

**Key words:** positron, back ground rejection, surgery

### INTRODUCTION

INTRA-OPERATIVE PROBES have recently become important instruments in nuclear medicine.<sup>1,2</sup> In such an application, the radiopharmaceutical F-18-fluorodeoxyglucose (FDG) is promising.<sup>1,3–5</sup> This positron emitter (FDG) can be detected by two methods in this application, one of which is the detection of beta particles while the other is the detection of annihilation gamma photons.<sup>6–12</sup> In both methods, it is difficult to distinguish the beta particles or

gamma photons from the background gamma photons because the background gamma photons have a high energy level (511 keV) that is similar to F-18 positrons. Detection of background gamma photons reduces the detectability of the tumor to normal ratio, making it difficult to apply the methods in clinical situations.

Several attempts have been made to overcome these limitations.<sup>10,13,14</sup> As one solution, we previously proposed a phoswich positron detector that uses a plastic scintillator to detect the beta particles, while the BGO detects gamma photons.<sup>15,16</sup> This configuration has also been applied to continuous blood sampling system and showed improved sensitivity to the conventional beta-detector-based system.<sup>17</sup> This time, we expanded the idea for an imaging detector using phoswich scintillators optically coupled to a multi-channel PSPMT. A similar detector has already been reported but with another

Received June 15, 2006, revision accepted September 25, 2006.

For reprint contact: Seiichi Yamamoto, Ph.D., Department of Electrical Engineering, Kobe City College of Technology, 8–3 Gakuen-Higashi-machi, Nishi-ku, Kobe 651–2194, JAPAN.

E-mail: s-yama@kobe-kosen.ac.jp

combination of scintillators and processing electronics.<sup>18</sup> In this paper we present the configuration and performance of our developed positron-imaging detector with background rejection capability.

## MATERIALS AND METHODS

### A. Principle of operation

Figure 1 shows a block diagram of the positron-imaging detector. The detector consists of an array of phoswich scintillators, optical fibers, a multi-channel PSPMT and a position-calculation and pulse-shape analysis circuit. Each phoswich scintillator consists of a plastic scintillator and a BGO and the scintillators and the PSPMT are optically coupled via optical fibers between them. These optical fibers are used to reduce the scintillation light spread to the neighboring channels of the PSPMT. They are encased in a tungsten shield, and replaceable collimators are mounted on the top of the detector.

Positrons are detected by the plastic scintillators while the annihilation photons, which are produced from the

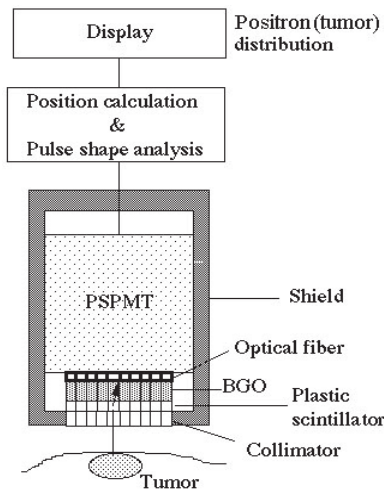


Fig. 1 Schematic diagram of the positron-imaging detector.

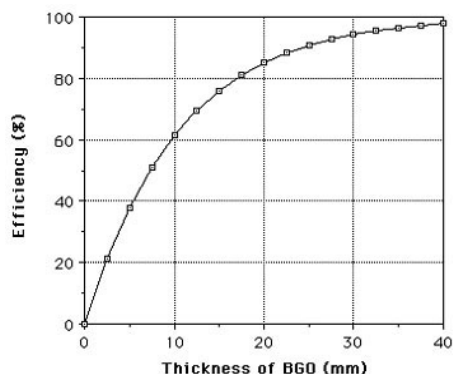


Fig. 2 Relation between thickness of BGO and detection efficiency for 511-keV gamma photons.

positrons in the plastic scintillators, are detected by the BGOs. If pulses are produced from both the plastic scintillator and the BGO simultaneously, the event is identified as a true positron event. If only one of these pulses is produced, the event is classed as a background event due to the annihilation gamma photons. By employing a pulse-shape analysis, we can distinguish the true events from background gamma events.<sup>15-17</sup> However, not all positrons absorbed in the plastic scintillator will result in annihilation photons that will travel in the correct direction to be detected by the BGO.

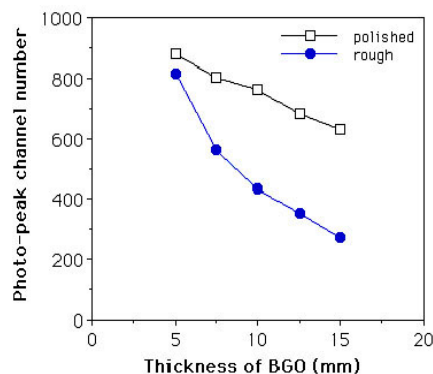


Fig. 3 Relation between thickness of the BGO and light output from a 2-mm square BGO for 511-keV.



Fig. 4 Photograph of phoswich scintillator, before optical coupling (left) and after optical coupling (right).

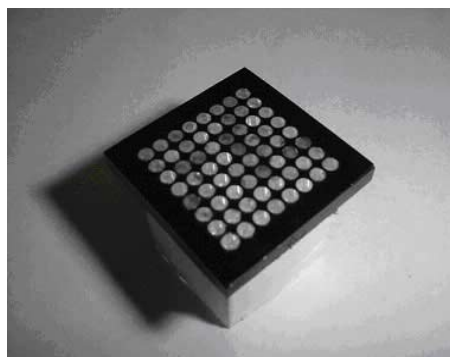


Fig. 5 Photograph of the optical fiber used between a phoswich scintillator array and a PSPMT.

### B. Phoswich detector

The dimensions of the plastic scintillator are 2 mm × 2 mm × 3 mm (BC-400, OKEN, Ibaragi, Japan). One reason why we selected the 3-mm thick plastic scintillator is that it is thick enough to absorb the full energy of positrons from F-18. An additional reason is that the plastic scintillator must absorb all the beta energy not to be detected by the BGO. If the plastic scintillator is thin and some fraction of the beta energy is detected by the BGO, the event may be detected as a true event by the system's electronics because both plastic scintillator and BGO produce signals.

Although a thicker BGO is better for the detection efficiency for annihilation photons, it also decreases the light output of the scintillation photons. Thus the optimum thickness of the BGO needs to be determined. We show the relation between thickness and detection efficiency of the BGO for annihilation photons calculated using a linear absorption coefficient of 0.95 (cm<sup>-1</sup>) for the BGO in Figure 2. We also measured the light output from 2-mm square BGOs of different lengths and surface treatments (rough and polished). Results are shown in Figure 3. These data were measured using 2-mm square BGOs of different length. Each BGO was optically coupled to a PMT and pulse height was measured for 511-keV gamma photons to estimate the light output. A Teflon™ (3M, USA) tape was used as the reflector.

With the rough surface, the light output decreased rapidly with increases in the thickness of the BGO. Using the 15-mm thick BGO with the polished surface, the light output was only 30% lower than that of the 5-mm one. Furthermore, the 15-mm BGO absorbed 75% of the annihilation photons. With these considerations, we determined the thickness of BGO to be 15 mm.

Figure 4 shows a photograph of a phoswich scintillator before and after optical coupling. Such scintillators are optically coupled to each other by optical cement (Bicon, BC-600), wrapped with Teflon tape and combined in an 8 × 8 array. The optically isolated phoswich scintillators act as light guides to transfer the scintillation light in the plastic scintillators to the PSPMT while maintaining the position information. The array is optically coupled to the 1-inch square 8 × 8 multi-channel PMT through optical fibers 2 mm in diameter 3 mm in thickness supported by a black plastic plate.

The optical fibers were employed to minimize the light spread of scintillation to neighbor channels of the PSPMT by its limited numerical aperture (N.A.). The optical fiber used was the Kuraray Clear-PCM type (N.A.; 0.72). Figure 5 shows a photograph of the optical fibers coupled on the phoswich scintillator array. Round optical fiber was selected because the material is used for reducing the light spread to adjacent channels. The round fiber can emit scintillation light in the central area of a single channel of the multi-channel PSPMT, although the light loss will be significant. Square fibers or a fiber-optic plate might be

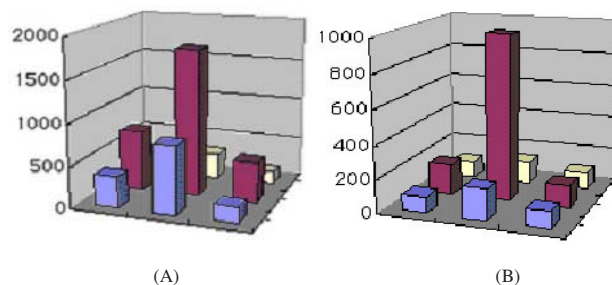


Fig. 6 Scintillation light distribution of one channel of the detector without the fiber (A) and with the fiber (B).

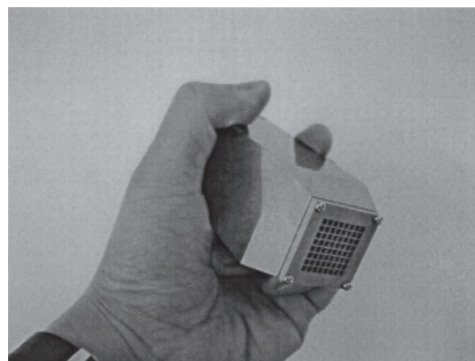


Fig. 7 Photograph of the developed positron-imaging detector.

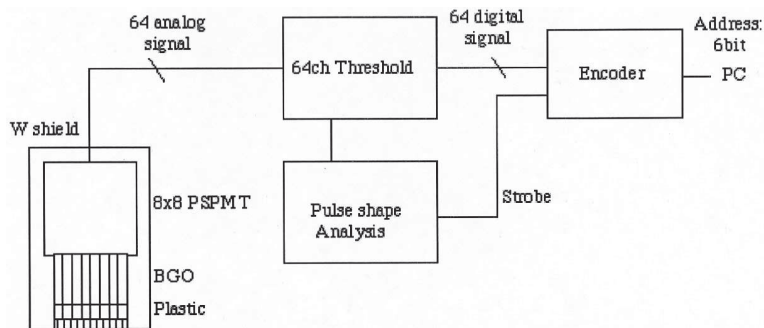
candidates for the material, but the light spread to neighbors may be greater even though the light loss is smaller.

Figure 6 shows the light spread to the adjacent channels of the BGO with and without the fibers measured for a typical channel of the PSPMT. These data were measured using a 2 mm × 2 mm × 15 mm BGO optically coupled to one channel of the PSPMT, and the signal amplitudes were measured for the channel and the eight adjacent channels with and without the fibers.

Without the fibers, the maximum light spread to adjacent channels was more than 40%, which makes it difficult to set low threshold levels. Using the optical fibers, the light spread to the adjacent channels fell to less than 20%. We also observed significant light loss from the fiber. The light loss resulting from using this fiber was approximately 40%. This phoswich array was optically coupled to a PSPMT. The PSPMT used was a Hamamatsu R 7548, 1-inch square, 8 × 8 multi-channel type.

### C. Detector configuration

In Figure 7 we show a photograph of the developed positron-imaging detector. The 8 × 8 phoswich scintillators and the PSPMT are encased in a tungsten shield. The tungsten shield absorbs the gamma photons from other parts of the body to reduce the count rate for the BGO. The thickness of this shield tapers from 3 mm to 8 mm at the input and is 3 mm around the remainder. The weight of the detector is approximately 1.5 kg. Although the weight is



**Fig. 8** Block diagram of the electronic circuit.

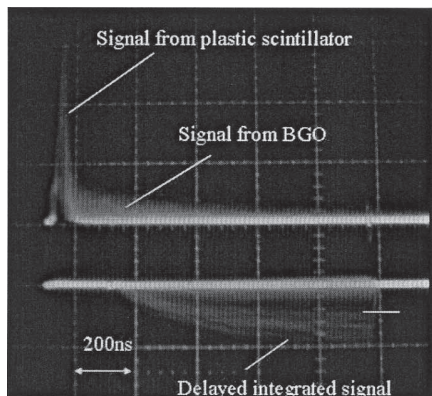


**Fig. 9** Photograph of the pulse shape of the detector (*top*) and the delayed integrated signal (*bottom*).

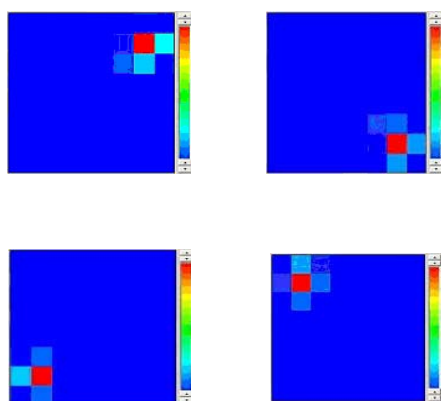


**Fig. 10** Images from the positron-imaging detector for an F-18 point source with 4 different positions.

not too heavy to be held in the hand of a surgeon, attempts may be needed to reduce the weight. One solution to reduce the weight of the detector is reduction of the thickness of the tungsten shield especially at the backside area where the scintillators are not located.

A detachable collimator is mounted on the top of the detector. This collimator is not necessary if the imaging detector can directly touch the tumor. However the collimator should be used because the input surface of the

imaging detector is covered by a thin light shield and is quite weak. Also in some of the clinical measurements, it is expected that the imaging detector will not be allowed to directly touch the patient. The collimator makes it possible to use the detector at a distance from the target but at the expense of a reduction of sensitivity.

The collimator was made of tungsten having  $8 \times 8$ , 2-mm square holes with 0.3-mm septa. The thickness of the collimator was 3 mm. The  $8 \times 8$  holes were positioned just above the  $8 \times 8$  phoswich scintillators of the imaging detector. The light shield for the input area was made of three layers of aluminum-vaporized Mylar film, each approximately 1 micrometer thick. The absorption of positron for F-18 was negligible for the Mylar films.

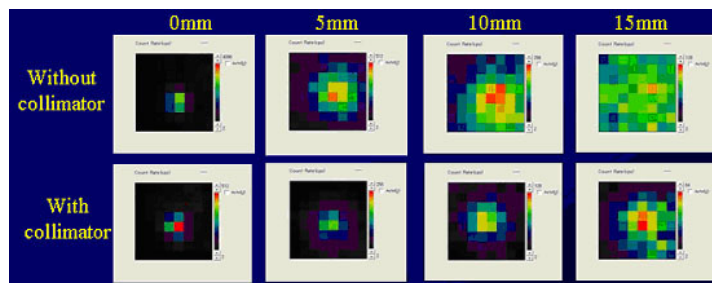
#### D. Electronic circuit

Figure 8 shows a block diagram of the electronic circuit of the position imaging detector. Position determination is performed by 64-channel threshold circuits. Position is determined only using the fast signal from the plastic scintillator, thus the BGO signal does not affect position determination even though the annihilation gamma photons were detected by the other detector element. Variable-gain amplifiers for gain control were used for all 64 channels. We used a summing signal of these 64-channel signals to analyze the pulse shapes based on the delayed integration method.

Figure 9 shows a photograph of the pulse shapes of the signals from the positron-imaging detector and the delayed integrated signal. The signal from the detector has two components; one is the fast signal from the plastic scintillator and the other is the slow component from the BGO. When the amplitude of the fast signal is larger than the threshold level, the signal is integrated after the fast pulse has decayed. When the amplitude of the delayed integrated signal is larger than the second threshold, the signal is a true count (positron). The other signals are recognized as background signals from annihilation gamma photons.

The threshold level for the fast signal was set to 30% of the peak level and that for the integrated signal was set to 70% of the peak level. These combinations were one of the optimum threshold settings for rejecting scattered





**Fig. 11** Images of the positron-imaging detector for a F-18 point source as a function of distance from the detector without (*top row*) and with collimator (*bottom row*).

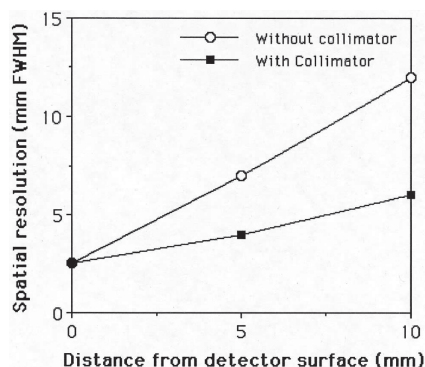


**Fig. 12** Spatial resolution as a function of the distance from the detector surface, measured with and without the collimator.

annihilation photons in the plastic scintillators.<sup>15</sup> Detected events are accumulated in the memory and transferred to a personal computer for display. A flood correction (divided by the flood image) is used to obtain the sensitivity corrected image.

## RESULTS

### A. Positioning property

Figure 10 shows images of the positron-imaging detector for a collimated F-18 point source with four different positions. Measurements were made using a collimated F-18 positron source positioned at each channel of the imaging detector. The size of the F-18 was around 2 mm and the activity was less than 37 kBq. Counts were only observed in the irradiated pixel. The spillover to the adjacent pixels was less than 20%. This spillover may have been mainly due to the size of the point source.

Figure 11 shows images of the positron-imaging detector for an F-18 point source as a function of distance from the detector surface. Measurements were made on an F-18 point source positioned above the imaging detector at 0 mm, 5 mm, 10 mm, and 15 mm from the detector surface. Data were measured without and with the collimator. Without the collimator, the point source was imaged as a point shape only on the detector surface (0 mm). With the collimator, the image of the point source was imaged as

point shape up to around 10 mm from the detector surface.

Figure 12 shows the relation between image resolution and distance from the detector surface with and without the collimator. Without the collimator, the image resolution degraded rapidly when the distance from the detector surface increased. With the collimator, the image resolution could be maintained at less than 6 mm FWHM up to 10 mm from the detector surface.

### B. Imaging property

The uniformity image of the positron-imaging detector is shown in Figure 13-(A). No flood correction was applied in this image. Measurement was made by uniformly irradiating positrons from F-18. Figure 13-(B) shows a profile of the image in the horizontal direction for two central pixels. Clearly, the sensitivity was higher at the central region of the detector and lower at the edges.

Figure 14-(A) and (B) respectively shows the dimensions and an image of the “H” phantom obtained by the positron imaging detector. The “H” phantom is made of 1-mm thick lead in the shape of an “H”. The phantom was positioned on the central pixels and positrons from F-18 were irradiated uniformly. The clear shape of “H” could be obtained with the phantom using the positron-imaging detector.

### C. Sensitivity

The sensitivity was measured by positioning an F-18 point source on the detector surface and measuring the count rates. The point source was made using an approximately 2-mm square piece of paper soaked in FDG solution. A thin plastic film was used to protect the detector surface from contamination. Measurements were made without and with the collimator at the central part of the detector surface where the sensitivity is highest. Results are shown in Figure 15. The sensitivity at the center was 1.4% (14 cps/kBq) without collimator and 0.25% (2.5 cps/kBq) with collimator.

### D. Background counts

In Figure 16, we show background count rates for a 20-cm diameter, 20-cm long phantom filled with F-18 with different activity levels. Measurements were made by

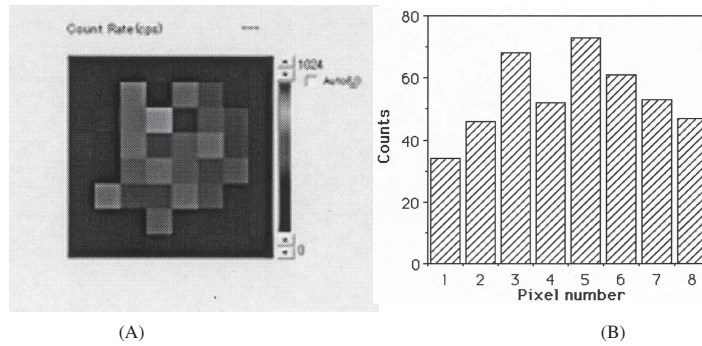


**Fig. 13** Image of the flood source of F-18 (A) and profile along the horizontal direction for two central pixels (B)

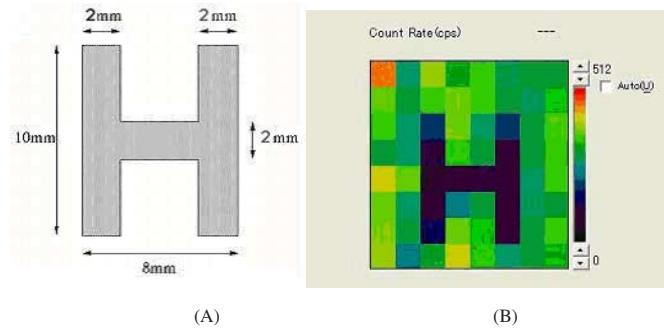


**Fig. 14** Dimension of the “H” phantom (A) and the image of the phantom obtained with the F-18 source (B).

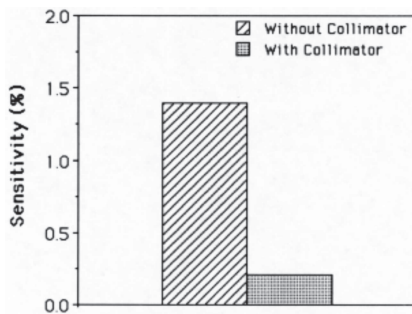


**Fig. 15** Sensitivity of the positron-imaging detector at the center of the detector surface for F-18 point source measured without and with the collimator.

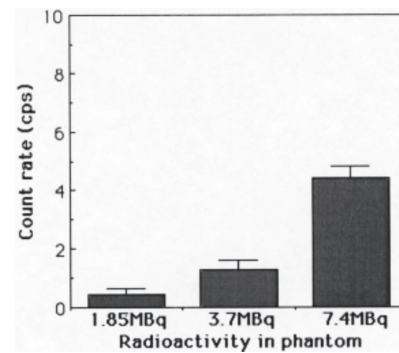


**Fig. 16** Background count rates for 20-cm diameter, 20-cm long phantom filled with F-18 of different activity levels.

positioning the positron-imaging detector on the central part of the phantom’s flat surface, and the count rates were recorded. Because the thickness of the phantom was more than 5 mm, all the positrons were absorbed in the phantom and only annihilation photons were detected by the positron-imaging detector. With an activity of 3.7 MBq, background counts were less than 2 cps.

In Figure 17, we show images of F-18 point sources with a 20-cm diameter, 20-cm long phantom filled with F-18 of different activity levels. Measurements were per-

formed with an F-18 point source at 100 kBq radioactivity positioned on one pixel of the position-imaging detector and set to the central region of the flat surface of the phantom. Images were recorded for 10 sec under each condition with the collimator mounted on the position-imaging detector. There were very small changes observed in the images between no activity (A) to 59.2 MBq in the phantom (G).

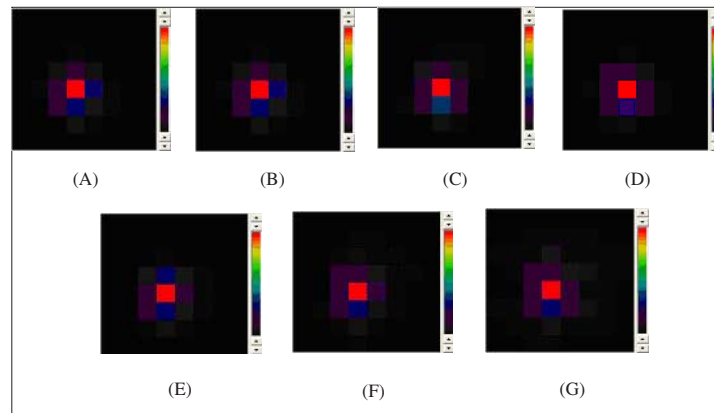


**Fig. 17** F-18 point source images with a 20-cm diameter, 20-cm long phantom filled with F-18 of different activity levels: (A) no activity, (B) 1.85 MBq in the phantom, (C) 3.7 MBq in the phantom, (D) 7.4 MBq in the phantom, (E) 14.8 MBq in the phantom, (F) 29.6 MBq in the phantom, (G) 59.2 MBq in the phantom.

## DISCUSSION AND CONCLUSION

We developed and tested a positron-imaging detector with background rejection capability for FDG-guided surgery. The sensitivity of the positron-imaging detector is determined by several factors. One is the detection efficiency of the plastic scintillator. For the imaging detector, the detection efficiency of the 3-mm plastic scintillator was 100%. Another is the detection efficiency of the BGO for the annihilation photons produced in the plastic scintillator. This reaches its minimum at the edges of the phoswich scintillators and its maximum in the central area. This effect was observed on the uniformity image shown in Figure 13. The threshold level for a fast signal in the electronic circuit is also related to the sensitivity; the signal of positrons lower than the threshold will be lost. The energy threshold for an integrated signal also experiences some loss of events due to signal variation in the channels, even though the amplitude of each channel was tuned to be the same. The input light shield affects the sensitivity loss if a thicker light shield is used. The aluminized Mylar films we employed, which were originally used for alpha-particle detectors, minimized the sensitivity loss.

One reason for the relatively low sensitivity of the developed positron imaging detector is the absorption of the F-18 positrons at the source. The point source used for the sensitivity measurement features self-absorption of the beta particles in the paper as well as in the FDG solution, while the radioactivity of the source was measured using a well counter based on the gamma photon measurements. Thus the F-18 positrons emitted from the point source might actually be smaller, leading to lower sensitivity of the imaging detector.

The sensitivity as the function of the distance from the detector surface was not measured in this study. This sensitivity property will be basically determined by the

solid angle of the detector surface from the point source. Without a collimator, the sensitivity will decrease as the distance is increased by the reduction of the solid angle. With a collimator, the sensitivity will be constant within some distance like the gamma camera sensitivity characteristic with a collimator.

The background counts measured using the cylindrical phantom containing the F-18 solution mainly came from accidental events of the signal from the plastic scintillator and BGO at high count rates. This accidental event rate is proportional to the count rate for the pulses from gamma detection by the plastic scintillators multiplied by that for the BGO. Thus, the accidental rate is proportional to the square of the background activity level. It may be possible to correct the accidental events using the delayed coincidence measurement, with some increases in complexity as well as the dead-time of the electronics.

The background counts also came from the pile-up events in the BGO. These pile-up events can be reduced by setting the narrow energy window for the integrated BGO signal. Moreover, the tungsten shield and collimator may contribute to reducing these background counts.

## ACKNOWLEDGMENTS

The authors wish to thank engineers of Espec Techno Co. for manufacturing the electronic circuits and software for the system. This work was partly supported by the Kansai Bureau, Ministry of Economy, Trade, and Industry, of Japan.

## REFERENCES

1. Hoffman EJ, Tornai MP, Janecek M, Patt BE, Iwanczyk JS. Intraoperative probes and imaging probes. *Eur J Nucl Med* 1999; 26 (8): 913–935.
2. Britten AJ. A method to evaluate intra-operative gamma probes for sentinel lymph node localization. *Eur J Nucl Med* 1999; 26 (2): 76–83.

3. Essner R, Hsueh EC, Haigh PI, Glass EC, Huynh Y, Daghighian F. Application of an F-18-fluorodeoxyglucose-sensitive probe for the intraoperative detection of malignancy. *J Surg Res* 2001; 96: 120–126.
4. Zervos EE, Desai DC, Depalatis LR, Soble D, Martin EW. F-18-labeled fluorodeoxyglucose positron emission tomography-guided surgery for recurrent colorectal cancer: a feasibility study. *J Surg Res* 2001; 97: 9–13.
5. Desai DC, Arnold M, Saha S, Hinkle G, Soble D, Fry J, et al. Correlative whole-body FDG-PET and intraoperative gamma detection of FDG distribution in colorectal cancer. *Clinical Positron Imaging* 2000; 3 (5): 189–194.
6. Lederman RJ, Raylman RR, Fisher SJ, Kison PV, San H, Nabel EG, et al. Detection of atherosclerosis using a novel positron-sensitive probe and 18-fluorodeoxyglucose (FDG). *Nucl Med Commun* 2001; 22 (7): 747–753.
7. Raylman RR, Wahl RL. A fiber-optically coupled positron-sensitive surgical probe. *J Nucl Med* 1994; 35 (5): 909–913.
8. Raylman RR, Wahl RL. Evaluation of ion-implanted-silicon detectors for use in intraoperative positron-sensitive probes. *Med Phys* 1996; 23 (11): 1889–1895.
9. Raylman RR, Fisher SJ, Brown RS, Ethier SP, Wahl RL. Fluorine 18-fluorodeoxyglucose-guided breast cancer surgery with a positron-sensitive probe: validation in preclinical studies. *Nucl Med* 1995; 36 (10): 1869–1874.
10. Raylman RR. Performance of a dual, solid-state intraoperative probe system with F-18, Tc-99m, and In-111. *J Nucl Med* 2001; 42 (2): 352–360.
11. Daghighian F, Mazziotta JC, Hoffman EJ, Shenderov P, Eshaghian B, Siegel S, et al. Intraoperative beta probe: a device for detecting tissue labeled with positron or electron emitting isotopes during surgery. *Med Phys* 1994; 21 (1): 153–157.
12. Yasuda S, Makuuchi H, Fujii H, Nakasaki H, Mukai M, Sadahiro S, et al. Evaluation of a surgical gamma probe for detection of <sup>18</sup>F-FDG. *Tokai J Exp Clin Med* 2000; 25 (3): 93–99.
13. Levin CS, Tornai MP, MacDonald LR, et al. Annihilation gamma ray background characterization and rejection for a small beta camera used for tumor localization during surgery. *IEEE Trans Nucl Sci* 1997; 44: 1120–1126.
14. Tornai MP, Levin CS, MacDonald LR, et al. A miniature phoswich detector for gamma-ray localization and beta imaging. *IEEE Trans Nucl Sci* 1998; 45: 1166–1173.
15. Yamamoto S, Matsumoto K, Senda M. Optimum threshold setting for a positron-sensitive probe with background rejection capability. *Ann Nucl Med* 2004; 18 (3): 251–256.
16. Yamamoto S, Matsumoto K, Senda M. An intra-operative positron probe with background rejection capability for FDG-guided surgery. *Ann Nucl Med* 2005; 19 (1): 23–28.
17. Yamamoto S, Tarutani K, Suga M, Minato K, Watabe H, Iida H. Development of a phoswich detector for a continuous blood sampling system. *IEEE Trans Nucl Sci* 2001; 48: 1408–1411.
18. Liu E, et al. Design and performance of a portable positron-sensitive surgical probe. Conference Records of IEEE Nuclear Science Symposium and Medical Imaging Conference, 2000.